

INDOOR COLLABORATIVE LOCALIZATION USING MULTIPLE MICRO-ELECTRO-MECHANICAL SYSTEM SENSOR NODES

YU LIU, TAIBAO JIANG*, YONGLE LU, XIN ZHANG AND YUNMEI LI

Chongqing Municipal Level Key Laboratory of Photoelectronic Information Sensing
and Transmitting Technology

Chongqing University of Posts and Telecommunications

No. 2, Chongwen Road, Nan'an Dist., Chongqing 400065, P. R. China

*Corresponding author: 18723126233@163.com

Received July 2016; accepted October 2016

ABSTRACT. *To address the challenge of real-time locating in complex indoor environments, we propose a novel scheme of indoor collaborative localization using multiple Micro-Electro-Mechanical System (MEMS) sensor nodes. The MEMS sensor node is modified and integrated with a Radio Frequency (RF) module which assists the node in communicating with the Base Station (BS). All the nodes can realize autonomous locating based on Pedestrian Dead Reckoning (PDR) algorithm, then transmit their latest position information to the BS to form real-time global topology and further achieve collaborative locating. We evaluate the proposed scheme in several indoor environments, and the experimental results demonstrate that the error ratio of locating among multiple nodes is 2.7%. Moreover, the proposed scheme requires less power and communication bandwidth, and it is practical for many relevant application fields.*

Keywords: Indoor cooperative localization, MEMS sensor, Inertial navigation, Pedestrian dead reckoning

1. Introduction. Recent years have witnessed the rapid development of mobile communication technologies, and the location-oriented techniques and services become more and more popular. Since there exist many unknown factors in some special indoor environments, such as fire escape and confined space which are out of the coverage of Global Positioning System (GPS) [1, 2], it has great difficulties in getting people's locations in these hostile environments. Thus, localizing people's positions in complex and dangerous indoor environment [3, 4, 5] receives lots of attention. For instance, in a burning building, if the fireman knows his exact position, he can evacuate as quickly as possible when critical events occur; or he can rescue his injured companions in time if he knows his companions' positions. This has important significance to the society.

Nowadays, domestic and foreign scholars have conducted a lot of researches on indoor localization. Two widely applicable localization techniques are Bluetooth based localization [6, 7, 8] and WiFi based localization [9]. Bluetooth based localization is suitable for close-distance scenario and its resolution lies in 3 ~ 5m, and Bluetooth usually has low penetrability which prevents it from locating people in different rooms. WiFi based localization involving wireless local area networks (WLANs) can realize small-scale localization, and it requires low cost and less base stations. However, WiFi signal is sensitive to external interference and needs higher transmission power compared with low-frequency signals, and it easily makes mistakes when locating different floors.

With the development of Micro-Electro-Mechanical System (MEMS), the size of sensors gets smaller and smaller and the cost keeps reducing, which fosters the MEMS sensor based inertial navigation technique. The inertial navigation technique can achieve high accuracy and has autonomy and continuity in the aspect of localization [10]. Since general MEMS

sensor nodes can only figure out their own positions, it is necessary to let every node have knowledge of others in the same space.

In this paper, we propose a novel indoor collaborative localization using multiple modified MEMS sensor nodes. The proposed scheme is based on the inertial navigation technique, and all the nodes are mounted with the 433 MHz radio frequency (RF) modules; the design diagram is shown in Figure 1. The nodes autonomously calculate their latest position by Pedestrian Dead Reckoning (PDR) and transmit the information to the Base Station (BS), and the BS gathers all the position information to form the global topology, which realizes collaborative localization among nodes. This achieves higher locating accuracy compared with Received Signal Strength Indicator (RSSI) based methods. Besides, considering that 433 MHz signals experience less transmission attenuation and have good ability of penetration and diffraction, they can travel longer distance compared with Bluetooth and WiFi signals, which extends the range of localization.

The rest of paper is organized as follows. We explain autonomous locating in Section 2 and introduce collaborative locating in Section 3. Section 4 describes the implementation and evaluates the results. We conclude our work in Section 5.

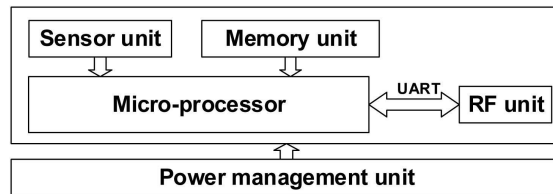


FIGURE 1. Design diagram of MEMS sensor node

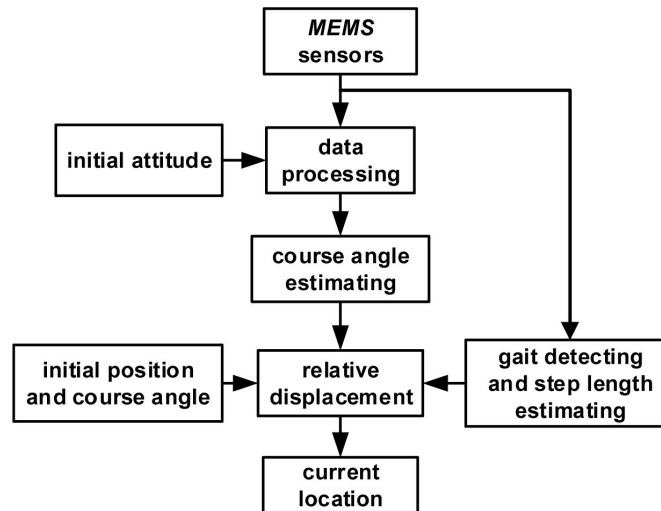


FIGURE 2. The basic process of PDR algorithm

2. Autonomous Locating. Given a known initial position, PDR utilizes the course angle and step length extracted from the MEMS sensors to calculate the relative displacement, and further locates the latest position of the pedestrian [11]. Figure 2 illustrates the basic process of PDR. The estimates of course angle and step length are shown as follows.

2.1. Course angle. Before calculating the course angle (expressed as γ), we need firstly get the pedestrian's pitch angle (expressed as α) and roll angle (expressed as β) from the 3-axis MEMS accelerometer, whose axes coincide with the pedestrian's carrier coordinate

axes. In carrier coordinate system, the output \mathbf{f}^b of 3-axis accelerometer can be expressed as

$$\mathbf{f}^b = [f_x^b \ f_y^b \ f_z^b]^T, \quad (1)$$

where f_x^b , f_y^b and f_z^b are three components of different axes, respectively. Moreover, in geographic coordinate system, the output is indicated as \mathbf{f}^n :

$$\mathbf{f}^n = [0 \ 0 \ g]^T, \quad (2)$$

where g is the measurement of gravitational acceleration. And the transformational relation between \mathbf{f}^b and \mathbf{f}^n is

$$\begin{bmatrix} f_x^b \\ f_y^b \\ f_z^b \end{bmatrix} = \begin{bmatrix} \cos \beta & \sin \beta \sin \alpha & -\sin \beta \cos \alpha \\ 0 & \cos \alpha & \sin \alpha \\ \sin \beta & -\cos \beta \sin \alpha & \cos \beta \cos \alpha \end{bmatrix} \begin{bmatrix} 0 \\ 0 \\ g \end{bmatrix}. \quad (3)$$

Therefore, pitch angle α and roll angle β can be calculated using the following equation:

$$\begin{aligned} \alpha &= \arctan \left(f_y^b / \sqrt{f_x^b + f_z^b} \right), \\ \beta &= \arctan \left(-f_x^b / f_z^b \right). \end{aligned} \quad (4)$$

In order to obtain the course angle γ , a 3-axis magnetometer is also needed and its axes coincide with the carrier coordinate axes. In carrier coordinate system, the magnetic strength reported from the magnetometer is expressed as

$$\mathbf{H}^b = [H_x^b \ H_y^b \ H_z^b]^T. \quad (5)$$

The magnetic strength components projected on the horizontal plane in geographic coordinate system can be transformed as

$$\begin{aligned} H_x^n &= H_x^b \cos \beta + H_z^b \sin \beta, \\ H_y^n &= H_x^b \sin \alpha \sin \beta + H_y^b \cos \alpha + H_z^b \sin \alpha \cos \beta. \end{aligned} \quad (6)$$

Thus, the course angle γ can be calculated with the following equation:

$$\gamma = \arctan (H_y^n / H_x^n). \quad (7)$$

2.2. Step length calculation. Step length calculation is based on the empirical model [12], which is formulated as

$$\begin{aligned} d_{step} &= C \sqrt[4]{A_{\max} - A_{\min}}, \\ C &= \frac{d_{real}}{d_{estimated}}, \end{aligned} \quad (8)$$

where A_{\max} and A_{\min} represent the maximum and minimum values of the accelerometer respectively in every step period, C is the calibration coefficient, d_{real} and $d_{estimated}$ separately denote the real value and estimated value of formerly statistical results and vary with different pedestrians.

We can adjust C and obtain accurate estimate of the step length for every specific pedestrian. The empirical model has low time complexity, which can help to reduce the response time of the system.

2.3. Single node position calculation. As it is shown in Figure 3, provided that the initial position is (x_0, y_0) , and the course angle and step length of the k th step are $d_{step}(k)$ and γ_k ($k = 1, 2, 3, \dots$), thus the current position (x_k, y_k) of the pedestrian can be written as

$$\begin{cases} x_k = x_0 + \sum_{i=1}^k d_{step}(i) \cos \gamma_i \\ y_k = y_0 + \sum_{i=1}^k d_{step}(i) \sin \gamma_i \end{cases}. \quad (9)$$

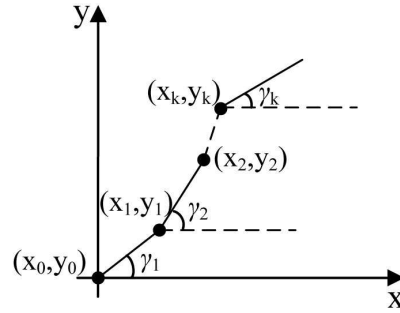


FIGURE 3. The principle of PDR

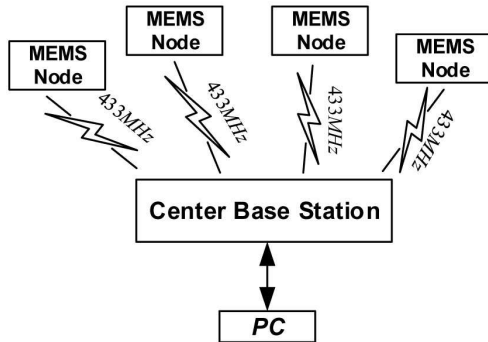


FIGURE 4. The communication between BS and each node

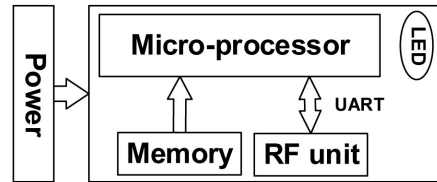


FIGURE 5. Design diagram of the BS

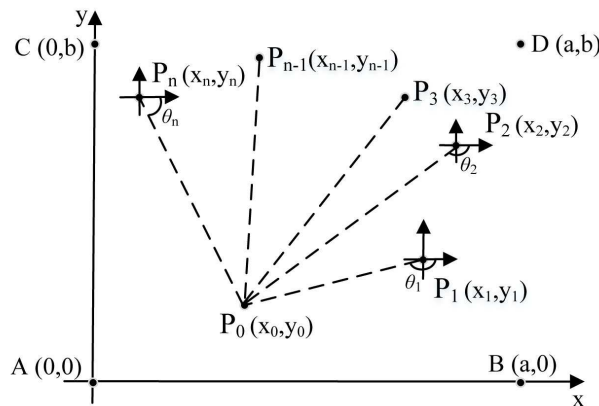


FIGURE 6. The global topology of n nodes

With the latest information of course angle and step length extracted from the MEMS sensors, every node can locate its own position in real time.

3. Collaborative Locating. To realize collaborative locating, one BS is required to collect the positions of all mobile nodes and form the global topology. The BS communicates with the MEMS nodes through the 433MHz wireless channel and reports information to the PC through a cable as shown in Figure 4. And the design diagram of the BS is illustrated in Figure 5.

The wireless network is built up in a self-organizing manner, and the global topology is updated in real time. As is shown in Figure 6, there exists $n + 1$ nodes in an $a \times b$ rectangular region, and the vertexes of the region are $A(0, 0)$, $B(a, 0)$, $C(0, b)$ and $D(a, b)$. At some time, the reported positions of n nodes are (x_0, y_0) , (x_1, y_1) , \dots , (x_{n-1}, y_{n-1}) and

(x_n, y_n) . Assume that the distances and drift angles between p_0 and other n nodes are d_1, d_2, \dots, d_n , and $\theta_1, \theta_2, \dots, \theta_n$, respectively. According to the following transformation:

$$\begin{bmatrix} d_1 & & & \\ & d_2 & & \\ & & \ddots & \\ & & & d_n \end{bmatrix} \begin{bmatrix} \cos \theta_1 & \sin \theta_1 \\ \cos \theta_2 & \sin \theta_2 \\ \vdots & \vdots \\ \cos \theta_n & \sin \theta_n \end{bmatrix} = \begin{bmatrix} x_1 - x_0 & y_1 - y_0 \\ x_2 - x_0 & y_2 - y_0 \\ \vdots & \vdots \\ x_n - x_0 & y_n - y_0 \end{bmatrix}, \quad (10)$$

$$\begin{bmatrix} d_1 \cos \theta_1 & d_1 \sin \theta_1 \\ d_2 \cos \theta_2 & d_2 \sin \theta_2 \\ \vdots & \vdots \\ d_n \cos \theta_n & d_n \sin \theta_n \end{bmatrix} = \begin{bmatrix} x_1 - x_0 & y_1 - y_0 \\ x_2 - x_0 & y_2 - y_0 \\ \vdots & \vdots \\ x_n - x_0 & y_n - y_0 \end{bmatrix}, \quad (11)$$

we can calculate the exact distances and drift angles of p_0 and other nodes. Therefore, every node can have the knowledge of others' positions using the global topology.

Since mobile nodes have the ability of autonomous locating and can communicate with the BS all the time as long as the links are connected, these all help to achieve accurate and large-scale collaborative localization in complex indoor environments.

4. Experiment and Evaluation.

4.1. Experiment setup. The MEMS sensor of every mobile node consists of one SCA3000-D01 capacitive accelerometer and one SMAG3 magnetometer, and the 16-bit MSP430F5438 micro-processor is selected for both mobile node and the BS. All the mobile nodes communicate with the BS using Si4432 RF chips through the 433MHz frequency band. A 3.3GHz Intel Core(TM) i5 CPU 8GB RAM laptop, which is used to generate global topology and record pedestrians' trajectories, connects with the BS by an RS232-to-USB cable.

Each mobile node is fixed to the lumbar spine of a person (shown in Figure 7), and we select two different sites, the No.1 teaching building and an underground parking of our campus, to conduct pedestrian walking test. The process of our proposed scheme is illustrated in Figure 8.

4.2. Single node locating test. We test single modified sensor node on the 50m \times 50m hollow-square corridor surrounding the classrooms of the No.1 teaching building and a 50m \times 50m region of the underground parking. There are more obstacles in the teaching building compared with that in the parking. The pedestrian stands at one vertex (initial position) of the square region and walks along the corridor or the edge of square, and his trajectories are recorded by the laptop as shown in Figure 9. We conduct the single node locating test for 10 times, and the results are listed in Table 1, where $d_{building}$ and $d_{parking}$ represent the estimated distances in teaching building and underground parking, respectively.



FIGURE 7. The mobile node is fixed to the lumbar spine of each pedestrian.

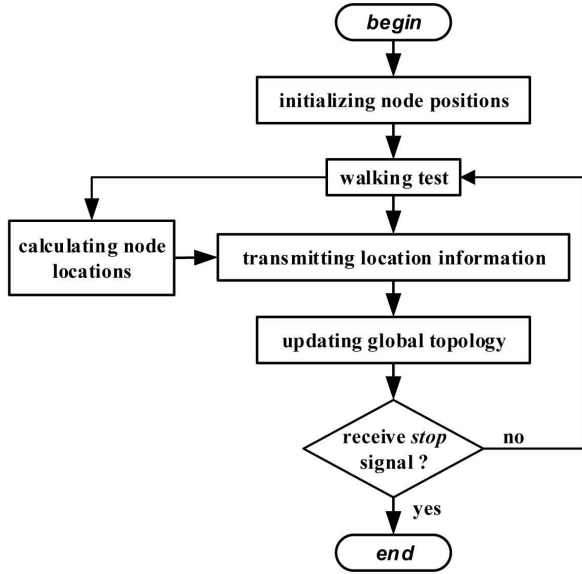


FIGURE 8. System processing flow

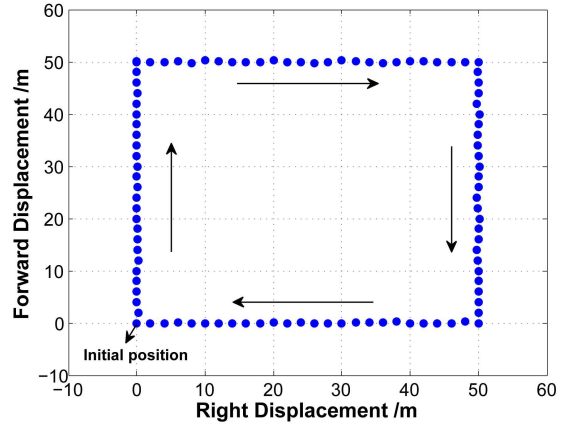


FIGURE 9. The pedestrian's trajectory in the parking

TABLE 1. Results of single node locating test

No.	True value (m)	$d_{parking}$ (m)	Error (m)	$d_{building}$ (m)	Error (m)
1	200	201.6	1.6	202.4	2.4
2	200	198.8	1.2	201.8	1.8
3	200	200.5	0.5	198.5	1.5
4	200	201.3	1.3	202.7	2.7
5	200	197.9	2.1	197.9	2.1
6	200	200.3	0.3	198.3	1.7
7	200	201.6	1.6	202.6	2.6
8	200	197.2	2.8	199.0	1.0
9	200	201.3	1.3	201.9	1.9
10	200	197.4	2.6	197.4	2.6

The average locating errors in the teaching building and the parking are 2.03m and 1.53m, respectively. Although the obstacles do have influence on locating, the error ratios are still lower than 1.5% while the error of GPS is about 5.0%. Thus, the proposed scheme is resilient to different indoor environments.

4.3. Multi-node collaborative locating test. The multi-node collaborative locating test is conducted on a $100\text{m} \times 100\text{m}$ square region of the underground parking. Four vertices are separately set as the initial positions of pedestrians $p_1 \sim p_4$, and the coordinates are $(0, 0)$, $(0, 100)$, $(100, 100)$ and $(100, 0)$. We evaluate the performance of collaborative locating from two aspects: walking along fixed path and unfixed path.

4.3.1. Walking along fixed path. The pedestrians are asked to walk along the edges of the square in clockwise direction, and stop when arriving at the next vertices. The test is conducted for 10 times. Figure 10 illustrates the trajectories of four pedestrians in one round, and the locating results are recorded in Table 2, where $d_1 \sim d_4$ separately denote the moving distances of pedestrians $p_1 \sim p_4$.

As shown in Table 2, the errors of all test rounds are lower than 3m and the totally average error is 2.19m.

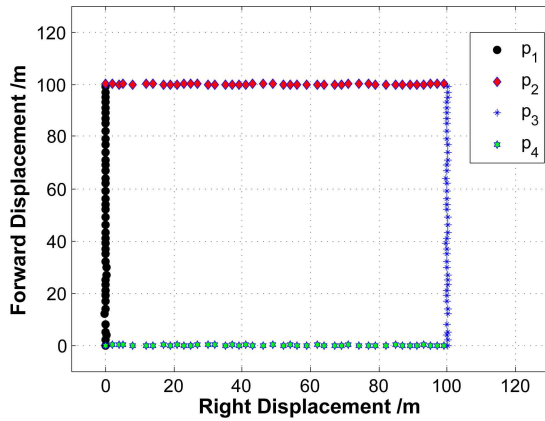


FIGURE 10. Walking along fixed path

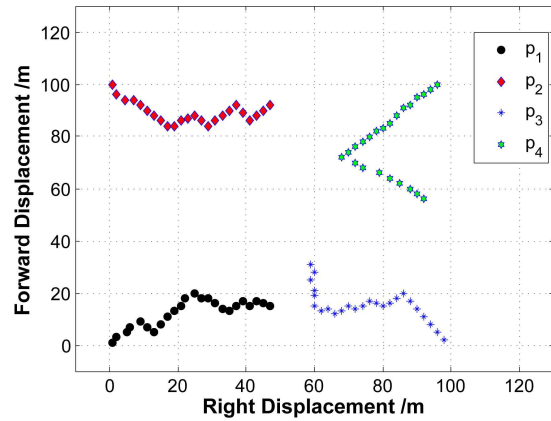


FIGURE 11. Walking along unfixed path

TABLE 2. Results of collaborative locating along fixed path

No.	True distance (m)	Estimated d_1 (m)	Estimated d_2 (m)	Estimated d_3 (m)	Estimated d_4 (m)	Average error (m)
1	100	102.4	98.4	101.7	100.5	1.6
2	100	101.8	102.7	103.1	98.8	2.2
3	100	98.5	104.0	101.5	102.9	2.5
4	100	103.7	99.2	95.7	102.1	2.7
5	100	97.9	101.9	100.5	98.7	1.5
6	100	99.3	104.1	102.0	103.3	2.5
7	100	102.6	96.8	101.9	99.0	2.2
8	100	99.0	103.0	98.8	97.1	2.2
9	100	101.9	102.9	98.6	103.4	2.4
10	100	97.4	102.1	103.7	99.4	2.3

TABLE 3. Results of collaborative locating along unfixed path

No.	True d_{12} (m)	Estimated d_{12} (m)	True d_{13} (m)	Estimated d_{13} (m)	True d_{14} (m)	Estimated d_{14} (m)	Average error (m)
1	64.0	61.2	55.2	57.8	82.8	80.4	2.6
2	60.6	59.8	71.5	70.1	49.9	48.5	1.2
3	62.1	60.8	58.7	60.8	72.3	71.1	1.5
4	54.7	52.4	59.4	62.8	35.1	34.7	2.0
5	66.5	67.6	49.2	47.6	84.5	82.9	1.4
6	43.1	42.7	62.7	61.3	56.5	55.1	1.1
7	47.4	48.8	33.8	32.9	69.6	67.4	1.5
8	62.3	60.7	60.2	58.7	61.1	64.3	2.1
9	44.8	46.1	69.0	66.2	35.4	34.8	1.6
10	57.2	56.3	68.3	66.7	75.8	77.1	1.3

4.3.2. *Walking along unfixed path.* In this test scenario, all pedestrians are asked to walk casually from their initial positions, and they are commanded to stop 5 minutes later. Their trajectories in one round are plotted in Figure 11, and the distances between pedestrian p_1 and other three pedestrians at the stop time are recorded in Table 3, where the true values are measured by a meter rule, d_{12} represents the distance between p_1 and p_2 , d_{13} represents the distance between p_1 and p_3 and so on.

The average error is 1.63m and the error ratio is 2.7%, which are acceptable in indoor localization.

5. Conclusion. In this work, we proposed a novel scheme of indoor collaborative locating using multiple mobile nodes. The node we made consists of an MEMS sensor and an RF module, and it can realize autonomous locating based on the pedestrian dead reckoning algorithm. In addition, every mobile node can transmit its real-time position information to the BS to form the global topology which helps the nodes have the knowledge of others. The experiments were conducted in several different scenarios, and the results demonstrated that the locating errors were lower than 3m and the error ratio of locating among multiple nodes is 2.7% in complex indoor environments. Since the cost of the proposed method is low and it needs less communication bandwidth, it is practical for many relevant fields.

We will continue to combine other efficient locating techniques to achieve much more accurate indoor localization in our future work.

Acknowledgment. We would like to thank all the anonymous reviewers for their comments. This work was funded in part by the National Natural Science Foundation of China (51175535).

REFERENCES

- [1] K. Badshah and Y. Qin, Tightly coupled integration of a low cost MEMS-INS/GPS system using adaptive Kalman filtering, *International Journal of Control and Automation*, vol.9, no.2, pp.179-190, 2016.
- [2] M. A. Rabbou and A. El-Rabbany, Tightly coupled integration of GPS precise point positioning and mems-based inertial systems, *GPS Solutions*, vol.19, no.4, pp.601-609, 2015.
- [3] Z. Zhou, T. Chen and L. Xu, An improved dead reckoning algorithm for indoor positioning based on inertial sensors, *International Conference on Electrical, Automation and Mechanical Engineering*, 2015.
- [4] J.-O. Nilsson, J. Rantakokko, P. Händel, I. Skog, M. Ohlsson and K. Hari, Accurate indoor positioning of firefighters using dual foot-mounted inertial sensors and inter-agent ranging, *IEEE/ION Position, Location and Navigation Symposium-PLANS*, pp.631-636, 2014.
- [5] X. Wang, S. Liu, C. Qin, J. Yuan and M. Lin, Real-time localization and information acquisition system based on wireless communication, *IEEE International Conference on Cyber Technology in Automation, Control, and Intelligent Systems*, pp.1293-1298, 2015.
- [6] S. Viswanathan and S. Srinivasan, Improved path loss prediction model for short range indoor positioning using bluetooth low energy, *SENSORS*, pp.1-4, 2015.
- [7] L. Chen, H. Kuusniemi, Y. Chen, L. Pei, T. Kröger and R. Chen, Information filter with speed detection for indoor bluetooth positioning, *International Conference on Localization and GNSS*, pp.47-52, 2011.
- [8] Y. Wang, X. Yang, Y. Zhao, Y. Liu and L. Cuthbert, Bluetooth positioning using RSSI and triangulation methods, *IEEE the 10th Consumer Communications and Networking Conference*, pp.837-842, 2013.
- [9] H. Zou, H. Jiang, X. Lu and L. Xie, An online sequential extreme learning machine approach to WiFi based indoor positioning, *IEEE World Forum on Internet of Things*, pp.111-116, 2014.
- [10] Z. Tian, Y. Zhang, M. Zhou and Y. Liu, Pedestrian dead reckoning for MARG navigation using a smartphone, *EURASIP Journal on Advances in Signal Processing*, vol.2014, no.1, p.1, 2014.
- [11] R. Ban, K. Kaji, K. Hiroi and N. Kawaguchi, Indoor positioning method integrating pedestrian dead reckoning with magnetic field and WiFi fingerprints, *The 8th International Conference on Mobile Computing and Ubiquitous Networking*, pp.167-172, 2015.
- [12] J. Jahn, U. Batzer, J. Seitz, L. Patino-Studencka and J. G. Boronat, Comparison and evaluation of acceleration based step length estimators for handheld devices, *International Conference on Indoor Positioning and Indoor Navigation*, pp.1-6, 2010.